Lifetime measurements of ^{17}C excited states and three-body and continuum effects

D. Smalley,[1] H. Iwasaki,[1,2] P. Navrátil,[3] R. Roth,[4] J. Langhammer,[4] V. M. Bader,[1,2] D. Bazin,[1] J. S. Berryman,[1,2] C. M. Campbell,[5] J. Dohet-Eraly,[3] P. Fallon,[5] A. Gade,[1,2] C. Langer,[1,6] A. Lemasson,[7] C. Loelius,[1,2] A. O. Macchiavelli,[5] C. Morse,[1,2] J. Parker,[8] S. Quaglioni,[9] F. Recchia,[1] S. R. Stroberg,[1,2] D. Weisshaar,[1] K. Whitmore,[1,2] and K. Wimmer[1,10]

[1]*National Superconducting Cyclotron Laboratory, Michigan State University, East Lansing, Michigan 48824, USA*

[2]*Department of Physics and Astronomy, Michigan State University, East Lansing, Michigan 48824, USA*

[3]*TRIUMF, 4004 Wesbrook Mall, Vancouver, British Columbia V6T 2A3, Canada*

[4]*Institüt fur Kernphysik, Technische Universität Darmstadt, 64289, Darmstadt, Germany*

[5]*Nuclear Science Division, Lawrence Berkeley National Laboratory, Berkeley, California 94720, USA*

[6]*Joint Institute for Nuclear Astrophysics, Michigan State University, East Lansing, Michigan 48824, USA*

[7]*Ganil, CEA/DSM-CNRS/IN2P3, Bd Henri Becquerel, BP 55027, F-14076 Caen Cedex 5, France*

[8]*Florida State University, Tallahassee, Florida 32306, USA*

[9]*Lawrence Livermore National Laboratory, P.O. Box 808, L-414, Livermore, California 94551, USA*

[10]*Department of Physics, Central Michigan University, Mount Pleasant, Michigan 48859, USA*

(Received 8 June 2015; revised manuscript received 13 October 2015; published 18 December 2015)

We studied transition rates for the lowest $1/2^+$ and $5/2^+$ excited states of ^{17}C through lifetime measurements with the GRETINA array using the recoil-distance method. The present measurements provide a model-independent determination of transition strengths giving the values of $B(M1;1/2^+ \rightarrow 3/2^+_{\text{g.s.}}) = 1.04^{+0.03}_{-0.12} \times 10^{-2}\mu_N^2$ and $B(M1;5/2^+ \rightarrow 3/2^+_{\text{g.s.}}) = 7.12^{+1.27}_{-0.96} \times 10^{-2}\mu_N^2$. The quenched $M1$ transition strength for the $1/2^+ \rightarrow 3/2^+_{\text{g.s.}}$ transition, with respect to the $5/2^+ \rightarrow 3/2^+_{\text{g.s.}}$ transition, has been confirmed with greater precision. The current data are compared to importance-truncated no-core shell model calculations addressing effects due to continuum and three-body forces.

DOI: 10.1103/PhysRevC.92.064314 PACS number(s): 21.10.Tg, 21.60.Cs, 23.20.−g, 27.20.+n

I. INTRODUCTION

Exotic nuclei with a large excess of neutrons exhibit properties distinct from nuclei close to stability, including the emergence of halo [1] and new deformation regions [2], and changes in shell closures [3–5]. These novel features can be traced to the underlying nucleon interaction and properties of weakly bound valence nucleons. Recent theoretical developments of large-scale shell model [6,7] and *ab initio* calculations [8–10] have demonstrated a possible link between these observed irregularities and fundamental properties of the nuclear interactions involving effects related to the tensor force [11] and the three-body force [12].

The neutron-rich carbon isotopes offer an intriguing basis to study the intricate effects of the nuclear forces through spectroscopy and lifetime measurements [13–22] as this region represents a frontier of current *ab initio* calculations including continuum and three-body forces. The anomalously long β-decay lifetime of ^{14}C [14] was found to have a microscopic origin attributed to the three-body force which induces a large cancellation of the Gamow-Teller strength within the p shell [23]. On the further neutron-rich side, recent γ-decay studies of ^{16,18}C [15,16] found that the effect of the three-body force was needed in order for their models to account for the observed branching ratios of the second 2^+ state.

As for odd-mass carbon isotopes, an exotic phenomenon associated with the strong $1s_{1/2}$ strength in the ground-state configuration has been observed in ^{15}C [24] and ^{19}C [17,21,25], where the latter is clearly identified as being a halo. In ^{17}C, the ground-state spin-parity (J^π) is determined to be $3/2^+_{\text{g.s.}}$ [18] despite the $J^\pi = 5/2^+$ naively expected from the conventional shell model. The occurrence of the low-lying $3/2^+$ state is consistent with other $N = 11$ or $Z = 11$ neighboring nuclei, and may also be ascribed to the effect of deformation as evidenced from the large cross section exciting the $5/2^+$ state at 331 keV in the (p,p') scattering [19]. The $1s_{1/2}$ strength in ^{17}C is manifested in the $1/2^+$ first excited state at 210 keV where the neutron knockout reaction from ^{18}C [20] exhibited a narrow momentum distribution characteristic of an s orbital.

A recent lifetime measurement of the excited states of ^{17}C [13] has suggested that the interplay between the $1/2^+$ halo state and the deformed $3/2^+_{\text{g.s.}}$ and $5/2^+$ states [19,22] induces the hindrance in the $1/2^+ \rightarrow 3/2^+_{\text{g.s.}}$ $M1$ transition strength. Later, it was shown in a shell model study that several corrections to the Suzuki-Fujimoto-Otsuka (SFO) Hamiltonian [26] are required to account for the reduction of the $1/2^+ \rightarrow 3/2^+_{\text{g.s.}}$ $M1$ transition and the correct ordering of the energy levels. The final effective interaction (SFO-tls) includes modifications to make the monopole matrix elements for the $\nu 0d_{5/2}-\nu 0d_{3/2}$ and $\nu 0d_{5/2}-\nu 1s_{1/2}$ more repulsive and the matrix elements $\nu 0d_{5/2}-\nu 0p_{3/2}$ and $\nu 0d_{5/2}-\nu 0p_{1/2}$ more attractive. It was later argued that the monopole interaction between the $\nu 0d_{5/2}$ and $\nu 0d_{3/2}$ orbitals derived from nucleon-nucleon (NN) forces is too attractive to reproduce the location of the oxygen drip line; however, the inclusion of three-body forces provides the additional repulsive contributions and resolves the discrepancy [27]. Therefore, the $T = 1$ monopole corrections introduced phenomenologically for the ^{17}C shell model calculations may have microscopic origins due to the three-body force.

In this work, we study transition rates through lifetime measurements and compare the results with *ab initio* importance-truncated no-core shell model (IT-NCSM) [8,9] calculations and importance-truncated no-core shell model with continuum (IT-NCSMC) [28] calculations to examine the effects of the three-body force along with considering the inclusion of the continuum due to the weakly bound nature of ^{17}C. Establishing experimental data on the electromagnetic transition strengths through direct lifetime measurements is essential to assessing and validating *ab initio* calculations. The previous lifetime measurements of the ^{17}C excited states [13] were performed using the recoil shadow method (RSM). Experimental uncertainties were 10% and 25% for the lifetimes of the $1/2^+$ and $5/2^+$ states, respectively. In this work, we employ the recoil-distance method (RDM) [29] coupled with the next-generation γ-ray tracking array, the Gamma-Ray Energy Tracking In-beam Nuclear Array (GRETINA) [30]. This setup is aimed at achieving the model-independent determination of the transition strengths with experimental errors of $\lesssim 10\%$ for both the excited states, which allows a rigorous comparison to the present no-core shell model calculations performed for the neutron-rich ^{17}C isotope.

The limiting factors for precision in the RDM studies with fast exotic beams are predominantly the yield in the γ-ray spectrum and the necessity for measurements with various distance settings. In order to overcome these limitations, we have employed the GRETINA array to exploit excellent efficiency and resolution for in-beam γ-ray spectroscopy. We have also developed a new plunger device, the triple plunger for exotic beams TRIple PLunger for EXotic beams (TRIPLEX) [31]. The new plunger design incorporates a target and two degrader foils allowing independent movement of the target and second degrader with respect to a fixed degrader in the middle. Two simultaneous RDM measurements can be performed with this new design which can provide two sensitive lifetime regions in a single experimental setup.

II. EXPERIMENT

The experiment was performed at the National Superconducting Cyclotron Laboratory (NSCL) at Michigan State University. A secondary beam of ^{18}C was produced by fragmentation of a ^{22}Ne primary beam at 120 MeV/nucleon incident on a 1480 mg/cm^2-thick ^{9}Be production target. The fragments were separated by the A1900 fragment separator [32] with a momentum acceptance of 2% and a 750 mg/cm^2 Al degrader wedge used to obtain about 90% beam purity for ^{18}C. The secondary beam was delivered to the reaction target with an energy of 74.2 MeV/nucleon at an average intensity of 2.9×10^4 pps where the one-neutron knockout reaction was used to populate the bound excited states in ^{17}C. Particle identification of reaction products was made by the S800 spectrograph [33] through the energy loss and time of flight measurements.

The plunger device was placed at the target position of the S800. This study relied on a 370 mg/cm^2 (2 mm) Be target plus two Ta degraders with thicknesses of 1640 mg/cm^2 (0.98 mm) and 950 mg/cm^2 (0.57 mm). The different velocity components for the ^{17}C reaction products through the plunger device were termed fast ($\beta_{\text{fast}} = 0.36$), reduced ($\beta_{\text{reduced}} = 0.31$), and slow ($\beta_{\text{slow}} = 0.27$) denoting the velocity after the target, first degrader, and second degrader, respectively. The distance between the target to first degrader (d_1) and first degrader to second degrader (d_2) was varied from 1 to 25 mm to provide characteristic γ-ray line shapes for determination of lifetimes in the range of 10 ps to 1 ns. Data were initially collected with the Be target only and then four different recoil-distance measurements were taken with the distances being $d_1 = 25$, $d_2 = 22.8$ mm; $d_1 = 5$, $d_2 = 22.8$ mm; $d_1 = 3$, $d_2 = 22.8$ mm; and $d_1 = 1$, $d_2 = 17.8$ mm. The largest distance data ($d_1 = 25$, $d_2 = 22.8$ mm) were taken to constrain the background contributions arising from the reactions in the degraders.

The deexcitation γ rays were detected with the GRETINA array [30]. The GRETINA detector module consists of four crystals each of which is divided into 36 segments. A total of seven detector modules were mounted with four detectors at forward angles ($25^\circ < \theta_{\text{lab}} < 55^\circ$) and three detectors at near 90° detection ($40^\circ < \theta_{\text{lab}} < 90^\circ$) with respect to the fixed first degrader of the plunger. In this study, the four detectors at forward angles were used exclusively for the lifetime measurement with a further angular cutoff applied ($\theta_{\text{lab}} < 40.0^\circ$). Excellent position resolution was obtained through the signal-decomposition algorithms [30] allowing a precise determination of the interaction point for use in Doppler-shift corrections. The momentum-vector information for particles was obtained on an event-by-event basis using the S800 and incorporated into the Doppler-shift correction. The plunger device was moved so that the center degrader was located 12.8 cm upstream with respect to the center of GRETINA in order to provide a balance between the γ-ray detection efficiency and the varying degrees of Doppler shifts due to the velocity change through each foil.

III. DATA ANALYSIS AND RESULTS

The γ-ray energy spectra of ^{17}C for three distance settings are shown in Fig. 1. The peaks for the $1/2^+ \rightarrow 3/2^+_{\text{g.s.}}$ and $5/2^+ \rightarrow 3/2^+_{\text{g.s.}}$ transitions are observed at 218 ± 1 and 332 ± 1 keV respectively. The γ-ray energies for each transition were determined experimentally with the target-only data taken prior to the insertion of the degrader foils. A χ-square minimization was performed to deduce the energy and errors. For the recoil-distance measurements, the Doppler-shift corrections are made by assuming γ-ray decay directly after the first degrader. Lifetime effects can be clearly observed in Fig. 1. This is seen through the reduction of the fast (f) components for both transitions as the distance between the target and degrader (d_1) is decreased from $d_1 = 25$ mm in Fig. 1(a), to $d_1 = 5$ mm in Fig. 1(b), and to $d_1 = 1$ mm in Fig. 1(c). For the $5/2^+ \rightarrow 3/2^+_{\text{g.s.}}$ transition an increase of the reduced (r) component can be observed as the distance d_1 decreases. The constant yields from the slow component indicate contributions from the reactions in the degraders. As for the $1/2^+ \rightarrow 3/2^+_{\text{g.s.}}$ transition, an increase is more significant for the slow (s) component which is indicative of a longer lifetime of the $1/2^+$ state compared to the previous state.

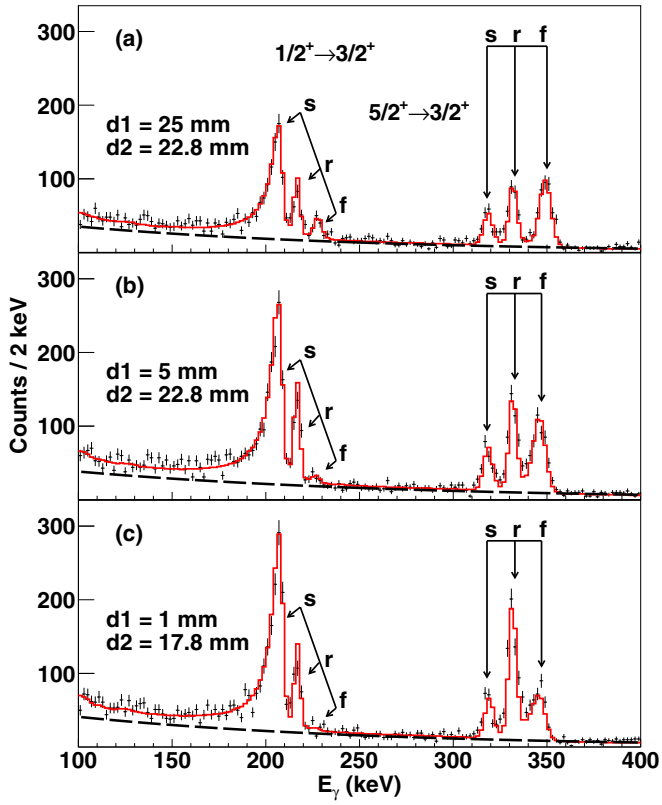

FIG. 1. (Color online) The observed γ rays of ^{17}C from the present RDM measurement with three different distance settings. The observed spectrum is overlaid with the simulated spectrum (solid histogram) which includes the exponential background (dashed curve). Identification of the fast (f), reduced (r), and slowed (s) components are shown.

We determined the lifetime with the least-squares method by comparing the data with simulations. In Fig. 1 the best-fit results for each distance setting are shown with the solid line being the total fit and the dashed line showing the exponential background. The simulations were based on existing GEANT4 code [34–36] with modifications to incorporate the GRETINA geometry. Beam characteristics of the incoming and outgoing particles are empirically constrained using experimental spectra and integrated into the code as inputs. Before determining the lifetime with the χ^2-minimization process, parameters for the exponential background and the degrader excitation contributions were required to be fixed using the data. The exponential background parameters were determined for each distance measurement individually from the measured data based on the continuous background regions in the spectra and fixed for the lifetime determination.

In order to constrain the degrader excitation contributions we first analyzed the longest distance data ($d_1 = 25$, $d_2 = 22.8$ mm). Two parameters are defined as R_t and R_d: R_t is the reaction ratio between the target and both degraders and R_d is the reaction ratio between the first and second degraders. The values of R_t and R_d were experimentally determined through a two-dimensional χ^2 hypersurface using spectra for the $5/2^+ \rightarrow 3/2^+_{\text{g.s.}}$ transition. For the $5/2^+$ state with a lifetime of $\tau \approx 20$ ps expected from Ref. [13], the flight time between foils, which corresponds to 200 ps at our beam velocity, is sufficient time for the excited states to decay prior to reaching the next foil. Therefore, the yield ratio between different Doppler-shift components observed in Fig. 1(a) provides a sensitive measure of R_t and R_d. This is not the case for the $1/2^+$ state which has a longer lifetime [13], thus the same values of R_t and R_d are assumed. The values of $R_t = 1.25^{+0.13}_{-0.12}$ and $R_d = 2.40^{+0.20}_{-0.24}$ were thus obtained in this work.

TABLE I. Summary of the present experimental data with a comparison to the previous $B(M1)$ results [13].

Transition	E_γ (keV)	τ (ps)	$B(M1)$ ($\times 10^{-2}\mu_N^2$) Present	Previous
$1/2^+ \rightarrow 3/2^+_{\text{g.s.}}$	218 ± 1	528^{+21}_{-14}	$1.04^{+0.03}_{-0.12}$	1.0 ± 0.1 [13]
$5/2^+ \rightarrow 3/2^+_{\text{g.s.}}$	332 ± 1	$21.8^{+3.4}_{-3.3}$	$7.12^{+1.27}_{-0.96}$	$8.2^{+3.2}_{-1.8}$ [13]

Present results of the mean lifetimes were determined to be $\tau = 528 \pm 11(\text{stat})^{+5}_{-0}(\text{sys}_{R_t})^{+5}_{-3}(\text{sys}_{R_d})$ ps and $\tau = 21.8 \pm 1.1(\text{stat})^{+1.8}_{-1.7}(\text{sys}_{R_t})^{+0.5}_{-0.5}(\text{sys}_{R_d})$ ps for the $1/2^+ \rightarrow 3/2^+_{\text{g.s.}}$ and the $5/2^+ \rightarrow 3/2^+_{\text{g.s.}}$ transitions, respectively. The largest source of uncertainty was attributed to the determination of R_t and R_d while other sources arising from beam optics and foil placement were evaluated to be negligible. For the $1/2^+ \rightarrow 3/2^+_{\text{g.s.}}$ transition it was found that R_t contributed only to an increase in the final lifetime measurement due to the characteristic line shape of the slow component strongly constraining the lifetime. By adding statistical and systematic errors we obtain the values of $\tau = 528^{+21}_{-14}$ ps for the $1/2^+ \rightarrow 3/2^+_{\text{g.s.}}$ transition and $\tau = 21.8^{+3.4}_{-3.3}$ ps for the $5/2^+ \rightarrow 3/2^+_{\text{g.s.}}$ transition as summarized in Table I.

In order to convert the measured lifetimes to $M1$ transition strengths, consideration of the $E2$ contributions is required. Even if we assume the strongest $E2$ transition of 100 Weisskopf units (W.u.) in this mass region [37], the $E2$ partial lifetime would still be far longer than the observed lifetimes: 780 ps for the $5/2^+ \rightarrow 3/2^+_{\text{g.s.}}$ transition and 6.5 ns for the $1/2^+ \rightarrow 3/2^+_{\text{g.s.}}$ transition due to the small level spacing. Therefore, a pure $M1$ transition can be safely assumed for the $5/2^+ \rightarrow 3/2^+_{\text{g.s.}}$ transition but possible uncertainty ($^{+47}_{-0}$ ps in the $M1$ partial lifetime) should be added to determine the $B(M1)$ value for the $1/2^+ \rightarrow 3/2^+_{\text{g.s.}}$ transition. The $B(M1)$ values are then determined to be $B(M1; 1/2^+ \rightarrow 3/2^+_{\text{g.s.}}) = 1.04^{+0.03}_{-0.12} \times 10^{-2}\mu_N^2$ and $B(M1; 5/2^+ \rightarrow 3/2^+_{\text{g.s.}}) = 7.12^{+1.27}_{-0.96} \times 10^{-2}\mu_N^2$. The current values are in good agreement with the previous measurement [13], but with greater precision, and they confirm the hindered transition of the 218-keV state.

IV. DISCUSSION

Precision $B(M1)$ measurements presented in this paper pose a challenge to nuclear theory. The ^{17}C is on the borderline of applicability of *ab initio* approaches such as the no-core shell model (NCSM) [10] in particular if three-body and continuum effects are incorporated. As the neutron-rich ^{17}C is weakly bound, it must be anticipated that continuum effects

will play a significant role and one has to be cautious when bound-state techniques such as the standard shell model or the IT-NCSM are applied. It is definitely preferable although extremely challenging to describe ^{17}C within the (IT-)NCSM with continuum that treats bound and unbound states in a unified framework [39]. Further, we learned from earlier investigation of the lighter ^{16}C [15] within the IT-NCSM that effects of the chiral three-nucleon ($3N$) interaction are manifest in the properties of the low-lying states of ^{16}C. Consequently, it is mandatory to include the chiral $3N$ in ^{17}C calculations, which further increases the complexity of the investigation. We note that so far the heaviest nucleus for which we were able to include both the continuum and the $3N$-force effects was ^{9}Be [28].

We have performed IT-NCSM and IT-NCSMC calculations for ^{17}C up to a model space size of $N_{\max} = 6$ with chiral $NN + 3N$ interactions [38,40,41], where results up to $N_{\max} = 6$ appear to be well under control for the extrapolation procedures used in the calculations. To assess the impact of the chiral $3N$ interaction, we also performed calculations using just the chiral NN interaction. In both cases, we employed the similarity renormalization group (SRG) transformations to soften the chiral interactions and improve the convergence. The SRG-induced $3N$ interaction has been taken into account in both cases.

To begin our investigation of the complex properties of ^{17}C we performed the IT-NCSM calculations with only the chiral NN interaction. The results of the calculated excitation energies are shown in Fig. 2(a). The correct level order is achieved at $N_{\max}$=2 but as $N_{\max}$ goes to 6 the calculation inverts the $1/2^+$ and $3/2^+$ states giving the incorrect level order. Since we have already observed the importance of the $3N$ force in ^{16}C we will now examine the effect that the $3N$ force has on the level order of the system.

The results of the calculated excitation energies of ^{17}C when adding the chiral $3N$ interaction are shown in Fig. 2(b). We find a sizable sensitivity to the presence of the $3N$ interaction. When it is taken into account the calculated excitation energies are in agreement with observed data concerning the level ordering, although the $1/2^+$ and $5/2^+$ states are higher by about 200 keV compared to experiment. We note, however, that the IT-NCSM calculations in the reachable basis sizes (up to $N_{\max} = 6$) predict ^{17}C to be unbound with respect to the ^{16}C $+n$ threshold as presented in Fig. 3. To further explore the influence of continuum effects due to the proximity to the threshold, we have performed the IT-NCSMC calculations with an extended basis that includes ^{16}C $+n$ binary cluster states computed with the ^{16}C ground state and the 2^+_1 state.

The excitation energies are compared for the IT-NCSM and IT-NCSMC in Fig. 3. The $NN + 3N$ interactions are used in both cases. We can see that without the continuum (IT-NCSM), ^{17}C remains unbound, but when the continuum is added ^{17}C becomes bound in the IT-NCSMC calculations. The S-wave dominated $1/2^+$ state shows the fastest convergence and becomes bound already in the $N_{\max} = 4$ basis while the $3/2^+$ and the $5/2^+$ states drop fast in energy, but a larger basis, beyond what we can reach at present, would still be needed for their binding. This behavior is in line with the

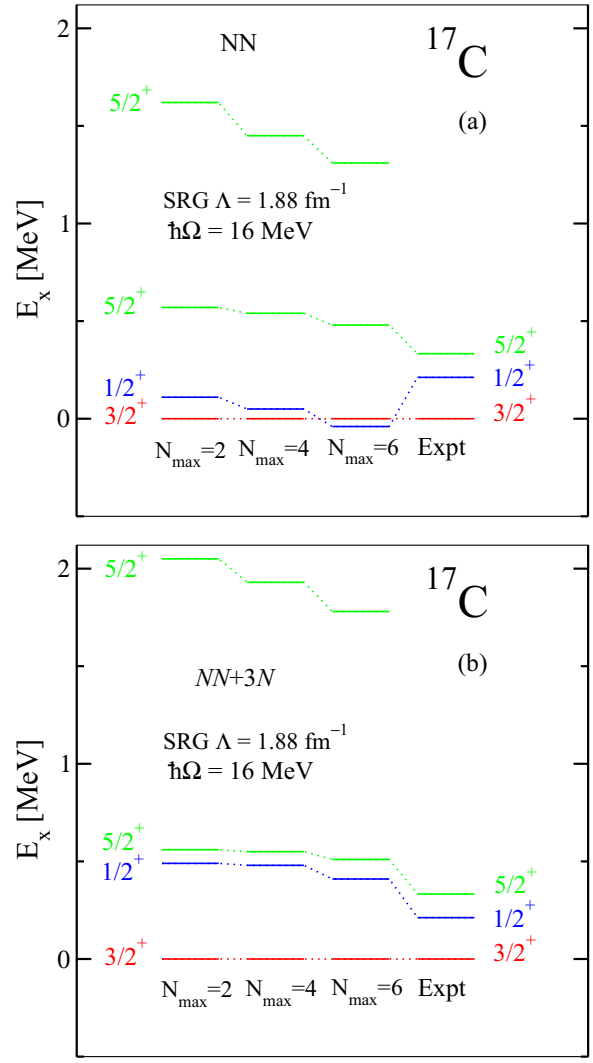

FIG. 2. (Color online) Calculated ^{17}C excitation energies for various basis sizes characterized by $N_{\max}$ compared to experiment. The IT-NCSM results obtained with the chiral NN interaction (labeled as NN) are shown in (a), while the calculations ($NN + 3N$) shown in (b) include the chiral $3N$ interaction with the 400 MeV/c cutoff [38].

general systematic for the variation in energies of the $s_{1/2}$ states relative to other states [42]. The energy change of the $s_{1/2}$ state close to the neutron thresholds is much less dramatic when compared to other states such as the $d_{5/2}$ with steeper energy changes. Since the $5/2^+$ and $3/2^+$ states are unbound within the current reach of the calculations, in this work, we are not able to calculate directly the $B(M1)$ values for the $5/2^+ \rightarrow 3/2^+$ and $1/2^+ \rightarrow 3/2^+$ transitions with the IT-NCSMC. However, we can modify our IT-NCSMC calculations in a phenomenological way by adjusting the NCSM input energies of the ^{16}C 2^+ and the ^{17}C $3/2^+$, $1/2^+$, and $5/2^+$ states to reproduce the experimental separation energies while still keeping untouched their corresponding wave functions. The result of this (now phenomenological) calculation is shown in the last column of Fig. 3 labeled as NCSMC-phenom. The lowest three states of ^{17}C are now

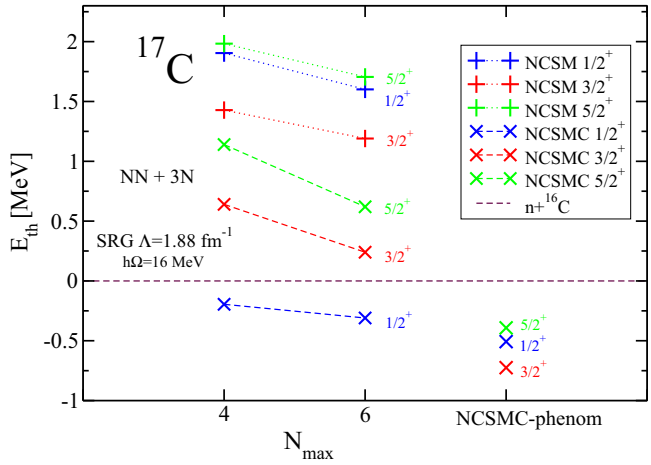

FIG. 3. (Color online) The IT-NCSM and the IT-NCSMC energies calculated using the chiral $NN+3N$ interactions are shown with respect to the ^{16}C$+n$ threshold. The HO frequency of $\hbar\Omega =$ 16 MeV that provides the fastest convergence is used. The energies calculated from the phenomenological IT-NCSMC calculations (NCSMC-phenom) at $N_{\max} = 6$ are also plotted. See text for further details.

all bound, allowing the investigation of $B(M1)$ transition strengths based on the IT-NCSMC framework.

Results of our IT-NCSM calculations of the $B(M1; 1/2^+ \rightarrow 3/2^+_{\text{g.s.}})$ and $B(M1; 5/2^+ \rightarrow 3/2^+_{\text{g.s.}})$ are illustrated in Fig. 4. First, we compare the calculations with and without the chiral $3N$ interaction to the present data. The calculated $B(M1; 1/2^+ \rightarrow 3/2^+_{\text{g.s.}})$ significantly

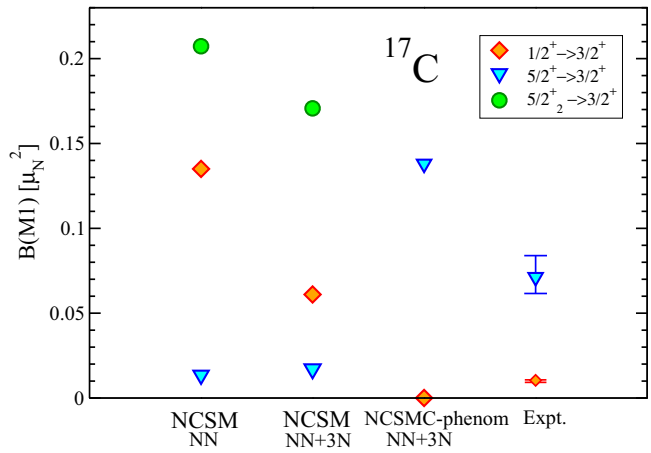

FIG. 4. (Color online) Calculated ^{17}C B(M1) transition rates with different theoretical approaches compared to the present experimental data. The IT-NCSM results obtained with the chiral NN and $NN+3N$ interactions with $N_{\max} = 4$ are plotted, where the calculated $B(M1)$ values appear to be stable with $N_{\max} = 2-6$. The $B(M1)$ calculations with the IT-NCSMC (NCSMC-phenom) were performed with $N_{\max} = 6$. The $5/2^+_2$ state is unbound in the NCSMC-phenom calculations and therefore the $B(M1)$ for the $5/2^+_2$ decay is not plotted. The standard one-body $M1$ operator with bare g factors was used. See Fig. 2 and the text for further details.

overestimates the experimental value in both cases, while the calculated $B(M1; 5/2^+_1 \rightarrow 3/2^+_{\text{g.s.}})$ underestimates the data by about a factor of 6. Clearly, the current NCSM calculations cannot reproduce the data. At the same time, we observe that the inclusion of the chiral $3N$ interaction moves the results in the direction of the experiment. These calculations were performed with bare g factors. In Fig. 4, we also show that the calculated $B(M1; 5/2^+_2 \rightarrow 3/2^+_{\text{g.s.}})$ values are slightly above the experimental $B(M1; 5/2^+_1 \rightarrow 3/2^+_{\text{g.s.}})$. It is possible to understand the NCSM results by calculating the spectroscopic factors of the ^{17}C eigenstates with respect to the ^{16}C$+n$ cluster states. For example, the $3/2^+_{\text{g.s.}}$ of ^{17}C has a large overlap with the ^{16}C$(2^+)+n$ in the S and, in particular, the D wave. On the contrary, the $5/2^+_1$ state is dominated by the ^{16}C$(0^+)+n$ in the D wave, which results in a strongly suppressed $M1$ transition. The $5/2^+_2$ state, on the other hand, has large spectroscopic factors in the ^{16}C$(2^+)+n$ channels similar to the $3/2^+_{\text{g.s.}}$ and, consequently, a strong $M1$ transition. The $1/2^+$ state in the NCSM calculation is a mixture of the ^{16}C$(0^+)+n$ in S wave and the ^{16}C$(2^+)+n$ in D wave, giving a non-negligible $M1$ transition.

In the phenomenologically adjusted IT-NCSMC calculation the structure of the ^{17}C bound eigenstates changes due to the inclusion of the continuum. In particular, the $1/2^+$ state ^{16}C$(0^+)+n$ S-wave component gets significantly enhanced and the $M1$ transition becomes strongly suppressed in agreement with the experimental observations. The situation is less transparent for the $5/2^+ \rightarrow 3/2^+$ transition. The $5/2^+$ bound state wave function receives an admixture of the $5/2^+_2$ NCSM eigenstate and the resulting $B(M1; 5/2^+ \rightarrow 3/2^+_{\text{g.s.}})$ gets significantly enhanced. The phenomenological IT-NCSMC $B(M1)$ results are qualitatively consistent with the present experimental measurement as seen in the last two columns of Fig. 4, indicating the importance of the continuum to account for the low-energy magnetic properties of ^{17}C.

V. CONCLUSION

In summary, the lifetimes of the first two excited states of ^{17}C were measured using the GRETINA array and the recoil-distance method. Excellent γ-ray position resolution obtained from the GRETINA signal decomposition routines allowed an unparalleled reconstruction of in-beam γ-ray data. The newly developed TRIPLEX plunger demonstrated the ability to simultaneously measure two lifetimes in the range of 10 ps to 1 ns with a single experimental setup. Our IT-NCSM and IT-NCSMC calculations demonstrate the importance of the chiral $3N$ interaction as well as the continuum for the binding of ^{17}C. While showing the necessity for large $N_{\max}$ calculations to bind all three ^{17}C states in these calculations, the phenomenological IT-NCSMC, which is based on the experimental binding energies of the ^{17}C states, enhances the S-wave component of the $1/2^+$ state close to the threshold and reproduces the suppressed $B(M1)$ for the $1/2^+$ decay. In particular, the present results suggest that continuum effects play a critical role for the understanding of the reported experimental $B(M1)$ values.

ACKNOWLEDGMENTS

The authors thank the beam physicists at the coupled cyclotron facility for the delivery of the radioactive beam. This work is supported by the National Science Foundation (NSF) (USA) under PHY-1102511, by the Department of Energy (DOE) National Nuclear Security Administration under award number DE-NA0000979. GRETINA was funded by the U.S. DOE Office of Science. Operation of the array at NSCL is supported by NSF under Cooperative Agreement PHY-1102511 (NSCL) and DOE under Grant No. DE-AC02-05CH11231 (LBNL). Numerical calculations have been performed at the LOEWE-CSC Frankfurt, and at the computing center of the TU Darmstadt (Lichtenberg). Computing support for this work also came in part from the LLNL institutional Computing Grand Challenge program and from an INCITE Award on the Titan supercomputer of the Oak Ridge Leadership Computing Facility (OLCF) at ORNL. Supported by the Deutsche Forschungsgemeinschaft through Contract SFB 634, by the Helmholtz International Center for FAIR (HIC for FAIR) within the LOEWE program of the State of Hesse, and the BMBF through Contract No. 06DA7047I, and from NSERC Grant No. 401945-2011. TRIUMF receives funding via a contribution through the National Research Council Canada. This work is supported in part by LLNL under Contract DE-AC52-07NA27344, and by the DOE, Office of Science, Office of Nuclear Physics, under Work Proposal No. SCW1158.

[1] I. Tanihata, H. Hamagaki, O. Hashimoto, Y. Shida, N. Yoshikawa, K. Sugimoto, O. Yamakawa, T. Kobayashi, and N. Takahashi, Phys. Rev. Lett. **55**, 2676 (1985).

[2] H. Scheit, T. Glasmacher, B. A. Brown, J. A. Brown, P. D. Cottle, P. G. Hansen, R. Harkewicz, M. Hellström, R. W. Ibbotson, J. K. Jewell, K. W. Kemper, D. J. Morrissey, M. Steiner, P. Thirolf, and M. Thoennessen, Phys. Rev. Lett. **77**, 3967 (1996).

[3] B. Bastin, S. Grevy, D. Sohler, O. Sorlin, Z. Dombradi, N. L. Achouri, J. C. Angelique, F. Azaiez, D. Baiborodin, R. Borcea, C. Bourgeois, A. Buta, A. Burger, R. Chapman, J. C. Dalouzy, Z. Dlouhy, A. Drouard, Z. Elekes, S. Franchoo, S. Iacob, B. Laurent, M. Lazar, X. Liang, E. Lienard, J. Mrazek, L. Nalpas, F. Negoita, N. A. Orr, Y. Penionzhkevich, Z. Podolyak, F. Pougheon, P. Roussel-Chomaz, M. G. Saint-Laurent, M. Stanoiu, I. Stefan, F. Nowacki, and A. Poves, Phys. Rev. Lett. **99**, 022503 (2007).

[4] H. Iwasaki *et al.*, Phys. Lett. B **491**, 8 (2000).

[5] T. Motobayashi *et al.*, Phys. Lett. B **346**, 9 (1995).

[6] T. Otsuka, Phys. Scr. **2013**, 014007 (2013).

[7] S. M. Lenzi, F. Nowacki, A. Poves, and K. Sieja, Phys. Rev. C **82**, 054301 (2010).

[8] R. Roth and P. Navrátil, Phys. Rev. Lett. **99**, 092501 (2007).

[9] R. Roth, Phys. Rev. C **79**, 064324 (2009).

[10] B. Barrett, P. Navrátil, and J. Vary, Prog. Part. Nucl. Phys. **69**, 131 (2013).

[11] T. Otsuka, T. Suzuki, R. Fujimoto, H. Grawe, and Y. Akaishi, Phys. Rev. Lett. **95**, 232502 (2005).

[12] O. Sorlin and M.-G. Porquet, Phys. Scr. **2013**, 014003 (2013).

[13] D. Suzuki *et al.*, Phys. Lett. B **666**, 222 (2008).

[14] S. Ruben and M. D. Kamen, Phys. Rev. **59**, 349 (1941).

[15] M. Petri, S. Paschalis, R. M. Clark, P. Fallon, A. O. Macchiavelli, K. Starosta, T. Baugher, D. Bazin, L. Cartegni, H. L. Crawford, M. Cromaz, U. DattaPramanik, G. deAngelis, A. Dewald, A. Gade, G. F. Grinyer, S. Gros, M. Hackstein, H. B. Jeppesen, I. Y. Lee, S. McDaniel, D. Miller, M. M. Rajabali, A. Ratkiewicz, W. Rother, P. Voss, K. A. Walsh, D. Weisshaar, M. Wiedeking, B. A. Brown, C. Forssen, P. Navratil, and R. Roth, Phys. Rev. C **86**, 044329 (2012).

[16] P. Voss, T. Baugher, D. Bazin, R. M. Clark, H. L. Crawford, A. Dewald, P. Fallon, A. Gade, G. F. Grinyer, H. Iwasaki, A. O. Macchiavelli, S. McDaniel, D. Miller, M. Petri, A. Ratkiewicz, W. Rother, K. Starosta, K. A. Walsh, D. Weisshaar, C. Forssen, R. Roth, and P. Navratil, Phys. Rev. C **86**, 011303 (2012).

[17] D. Bazin, B. A. Brown, J. Brown, M. Fauerbach, M. Hellstrm, S. E. Hirzebruch, J. H. Kelley, R. A. Kryger, D. J. Morrissey, R. Pfaff, C. F. Powell, B. M. Sherrill, and M. Thoennessen, Phys. Rev. Lett. **74**, 3569 (1995).

[18] V. Maddalena, T. Aumann, D. Bazin, B. A. Brown, J. A. Caggiano, B. Davids, T. Glasmacher, P. G. Hansen, R. W. Ibbotson, A. Navin, B. V. Pritychenko, H. Scheit, B. M. Sherrill, M. Steiner, J. A. Tostevin, and J. Yurkon, Phys. Rev. C **63**, 024613 (2001).

[19] Z. Elekes *et al.*, Phys. Lett. B **614**, 174 (2005).

[20] Y. Kondo, T. Nakamura, Y. Satou, T. Matsumoto, N. Aoi, N. Endo, N. Fukuda, T. Gomi, Y. Hashimoto, M. Ishihara, S. Kawai, M. Kitayama, T. Kobayashi, Y. Matsuda, N. Matsui, T. Motobayashi, T. Nakabayashi, K. Ogata, T. Okumura, H. J. Ong, T. K. Onishi, H. Otsu, H. Sakurai, S. Shimoura, M. Shinohara, T. Sugimoto, S. Takeuchi, M. Tamaki, Y. Togano, and Y. Yanagisawa, Phys. Rev. C **79**, 014602 (2009).

[21] K. Whitmore, D. Smalley, H. Iwasaki, T. Suzuki, V. M. Bader, D. Bazin, J. S. Berryman, B. A. Brown, C. M. Campbell, P. Fallon, A. Gade, C. Langer, A. Lemasson, C. Loelius, A. O. Macchiavelli, C. Morse, T. Otsuka, J. Parker, F. Recchia, S. R. Stroberg, D. Weisshaar, and K. Wimmer, Phys. Rev. C **91**, 041303 (2015).

[22] H. Sagawa, X. R. Zhou, T. Suzuki, and N. Yoshida, Phys. Rev. C **78**, 041304 (2008).

[23] P. Maris, J. P. Vary, P. Navratil, W. E. Ormand, H. Nam, and D. J. Dean, Phys. Rev. Lett. **106**, 202502 (2011).

[24] A. Ozawa, T. Kobayashi, T. Suzuki, K. Yoshida, and I. Tanihata, Phys. Rev. Lett. **84**, 5493 (2000).

[25] T. Nakamura, N. Fukuda, T. Kobayashi, N. Aoi, H. Iwasaki, T. Kubo, A. Mengoni, M. Notani, H. Otsu, H. Sakurai, S. Shimoura, T. Teranishi, Y. X. Watanabe, K. Yoneda, and M. Ishihara, Phys. Rev. Lett. **83**, 1112 (1999).

[26] T. Suzuki and T. Otsuka, Phys. Rev. C **78**, 061301 (2008).

[27] T. Otsuka, T. Suzuki, J. D. Holt, A. Schwenk, and Y. Akaishi, Phys. Rev. Lett. **105**, 032501 (2010).

[28] J. Langhammer, P. Navrátil, S. Quaglioni, G. Hupin, A. Calci, and R. Roth, Phys. Rev. C **91**, 021301 (2015).

[29] A. Dewald, O. Mller, and P. Petkov, Prog. Part. Nucl. Phys. **67**, 786 (2012).

[30] S. Paschalis *et al.*, Nucl. Instrum. Methods Phys. Res., Sect. A **709**, 44 (2013).

[31] H. Iwasaki *et al.*, Nucl. Instrum. Methods Phys. Res., Sect. A **806**, 123 (2016).

[32] D. J. Morrissey *et al.*, Nucl. Instrum. Methods Phys. Res., Sect. B **204**, 90 (2003).
[33] D. Bazin *et al.*, Nucl. Instrum. Methods Phys. Res., Sect. B **204**, 629 (2003).
[34] S. Agostinelli *et al.*, Nucl. Instrum. Methods Phys. Res., Sect. A **506**, 250 (2003).
[35] P. Adrich *et al.*, Nucl. Instrum. Methods Phys. Res., Sect. A **598**, 454 (2009).
[36] A. Lemasson, H. Iwasaki, C. Morse, D. Bazin, T. Baugher, J. S. Berryman, A. Dewald, C. Fransen, A. Gade, S. McDaniel, A. Nichols, A. Ratkiewicz, S. Stroberg, P. Voss, R. Wadsworth, D. Weisshaar, K. Wimmer, and R. Winkler, Phys. Rev. C **85**, 041303 (2012).
[37] P. Endt, At. Data Nucl. Data Tables **55**, 171 (1993).
[38] R. Roth, S. Binder, K. Vobig, A. Calci, J. Langhammer, and P. Navrátil, Phys. Rev. Lett. **109**, 052501 (2012).
[39] S. Baroni, P. Navrátil, and S. Quaglioni, Phys. Rev. Lett. **110**, 022505 (2013).
[40] D. R. Entem and R. Machleidt, Phys. Rev. C **68**, 041001 (2003).
[41] P. Navrátil, Few-Body Syst. **41**, 117 (2007).
[42] C. R. Hoffman, B. P. Kay, and J. P. Schiffer, Phys. Rev. C **89**, 061305 (2014).